Available online at www.sciencedirect.com
ScienceDirect
Journal of Colloid and Interface Science 315 (2007) 607–619
JOURNAL OF Colloid and Interface Science
www.elsevier.com/locate/jcis

Water in oil emulsion droplet size characterization using a pulsed field gradient with diffusion editing (PFG-DE) NMR technique

Clint P. Aichele *, Mark Flaum, Tianmin Jiang, George J. Hirasaki, Walter G. Chapman

Department of Chemical and Biomolecular Engineering, Rice University, 6100 Main St., Houston, TX 77005, USA

Received 13 February 2007; accepted 14 July 2007

Available online 28 July 2007

Abstract

This paper describes a proton nuclear magnetic resonance (NMR) technique, pulsed field gradient with diffusion editing (PFG-DE), to quantify drop size distributions of brine/crude oil emulsions. The drop size distributions obtained from this technique were compared to results from the traditional pulsed field gradient (PFG) technique. The PFG-DE technique provides both transverse relaxation (T_2) and drop size distributions simultaneously. In addition, the PFG-DE technique does not assume a form of the drop size distribution. An algorithm for the selection of the optimal parameters to use in a PFG-DE measurement is described in this paper. The PFG-DE technique is shown to have the ability to resolve drop size distributions when the T_2 distribution of the emulsified brine overlaps either the crude oil or the bulk brine T_2 distribution. Finally, the PFG-DE technique is shown to have the ability to resolve a bimodal drop size distribution.
Published by Elsevier Inc.

Keywords: Petroleum; Emulsions; NMR; Drop size distribution

1. Introduction

Emulsions are dispersions of one liquid in another, immiscible liquid. In the petroleum industry, brine/crude oil emulsions can potentially form during crude oil production [1]. Typically, brine/crude oil emulsions are not preferred during crude oil production because of processing issues [2]. However, brine/crude oil emulsions can be beneficial in some cases, such as in the prevention of methane hydrate blockages [3–5]. Specifically, the drop size distributions of brine/crude oil emulsions can be used to understand and quantify emulsion formation and stability mechanisms. Therefore, knowledge of the drop size distribution of an emulsion aids in manipulating the emulsion to a desired condition. This paper addresses techniques used to measure drop size distributions of brine/crude oil emulsions using proton nuclear magnetic resonance (NMR). This work focuses on petroleum emulsions; however, this technique could also be used to investigate emulsions in the food and pharmaceutical industries.

Historically, researchers have attempted to measure drop size distributions of emulsions using techniques including microscopy, light scattering, Coulter counting, and nuclear magnetic resonance [6–8]. For brine/crude oil emulsions, nuclear magnetic resonance is a superior technique because it is not destructive to the emulsion, it considers the entire sample, and it is not restricted by the fact that brine/crude oil emulsions do not transmit an appreciable amount of light. Traditionally, NMR has been used to measure drop size distributions of emulsions according to the technique developed by Packer and Rees [9]. The Packer–Rees technique incorporates the idea of restricted diffusion established by Neuman [10] and refined by Murday and Cotts [11] for diffusion in spheres.

The method presented by Packer and Rees relies on the assumption that the drops in emulsions are distributed in size according to the lognormal distribution. This restriction often results in the loss of valuable information about the actual emulsion drop size distribution. Therefore, techniques have been developed and discussed in the literature that are designed to yield more general information about drop size distributions of emulsions, independent of the assumption that the drops are lognormally distributed [12].

* Corresponding author.
E-mail address: clinta@rice.edu (C.P. Aichele).

0021-9797/$ – see front matter Published by Elsevier Inc.
doi:10.1016/j.jcis.2007.07.057

This paper presents a new technique that provides both the T_2 and drop size distributions of brine/crude oil emulsions simultaneously. This paper also presents an algorithm that can be used to calculate parameters for both PFG-DE and PFG experiments for a variety of emulsion conditions. The PFG-DE technique involves a two-dimensional inversion with regularization much like that used for obtaining diffusivity and transverse relaxation information [13–15]. The drop size distributions obtained from the PFG-DE technique are compared to drop size distributions obtained from the stimulated echo pulsed field gradient (PFG) technique [6,16]. In this paper, the PFG-DE technique is shown to be useful for obtaining drop size distributions when the T_2 distribution of the emulsified brine overlaps either the bulk brine or crude oil T_2 distribution. Finally, the utility of the PFG-DE technique is particularly observed when the drop size distribution of the emulsion is more complicated, such as when the distribution is bimodal.

2. Experimental methods

The proton NMR measurements discussed in this paper were performed on a 2 MHz Maran Ultra spectrometer that was maintained at $30 \pm 0.1\,^{\circ}\mathrm{C}$. The following sections contain the pulse sequences and experimental methods that were used in this work.

2.1. Carr–Purcell–Meiboom–Gill (CPMG)

Fig. 1 illustrates the Carr–Purcell–Meiboom–Gill (CPMG) pulse sequence that can be used to obtain transverse relaxation information about an emulsion sample [17,18].

After obtaining the T_2 distribution, the resulting drop size distribution can be determined according to Eq. (1) [6]

$$d_i = 6\rho\left(\frac{1}{T_{2,i}} - \frac{1}{T_{2,\mathrm{bulk}}}\right)^{-1}. \tag{1}$$

The surface relaxivity, ρ, is determined either by combining a CPMG and PFG measurement [12] or by performing a PFG-DE measurement. The bulk transverse relaxation time of the fluid that is confined in the drops is given by $T_{2,\mathrm{bulk}}$. The CPMG measurement is fast with duration usually equal to 10 min. Most importantly, the shape of the drop size distribution obtained from the CPMG technique is not assumed. For these reasons, Eq. (1) is useful for determining drop size distributions of emulsions when the transverse relaxation distribution of the emulsified brine is separated from both the crude oil distribution and the bulk brine distribution.

2.2. Pulsed field gradient (PFG)

The pulsed field gradient (PFG) stimulated echo technique has been shown to facilitate the characterization of emulsion drop size distributions [6,16].

Fig. 2 shows the pulsed field gradient pulse sequence with stimulated echoes and pre-gradient pulses. Three to nine pre-gradient pulses should be used to make the final two gradient pulses identically shaped. In the work discussed in this paper, the gradient strength values were manipulated in each experiment to facilitate attenuation of the emulsion signal. The amplitude of the first echo was obtained by linearly fitting the amplitudes of the first ten echoes, thereby increasing the signal:noise ratio (SNR) of the measurement.

The attenuation decay in a PFG measurement is coupled with the model developed by Murday and Cotts [11] for diffusion in spheres to obtain the drop size distribution of the emulsion. The model for attenuation of the signal of fluid confined in spheres is given by Eqs. (2)–(4) [10,11]:

$$R_{\mathrm{sp}} = \exp\left\{-2\gamma_g^2 g^2 \sum_{m=1}^{\infty} \frac{1}{\alpha_m^2(\alpha_m^2 r^2 - 2)} \times \left[\frac{2\delta}{\alpha_m^2 D_{\mathrm{DP}}} - \frac{\Psi}{(\alpha_m^2 D_{\mathrm{DP}})^2}\right]\right\}, \tag{2}$$

$$\Psi = 2 + \exp\left(-\alpha_m^2 D_{\mathrm{DP}}(\Delta - \delta)\right) - 2\exp\left(-\alpha_m^2 D_{\mathrm{DP}}\delta\right) - 2\exp\left(-\alpha_m^2 D_{\mathrm{DP}}\Delta\right) + \exp\left(-\alpha_m^2 D_{\mathrm{DP}}(\Delta + \delta)\right). \tag{3}$$

The gyromagnetic ratio is given by γ_g, the gradient strength is g, D_{DP} is the diffusivity of the fluid in the dispersed phase, r is the radius of the emulsion droplet, Δ is the time between gradient pulses, δ is the gradient pulse duration, and α_m is the mth positive root of

$$\frac{1}{\alpha r} J_{3/2}(\alpha r) = J_{5/2}(\alpha r). \tag{4}$$

J_k is the Bessel function of the first kind with order k. The overall attenuation of the emulsion has been shown to be a function of the attenuation of both the continuous and dispersed

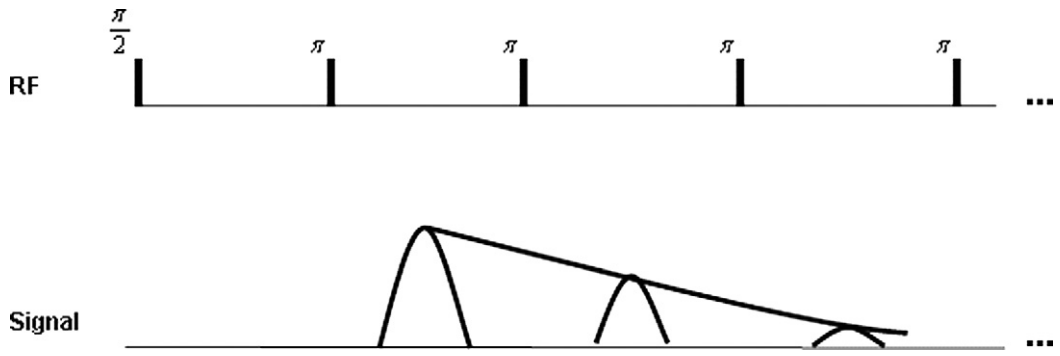

Fig. 1. Carr–Purcell–Meiboom–Gill (CPMG) pulse sequence.

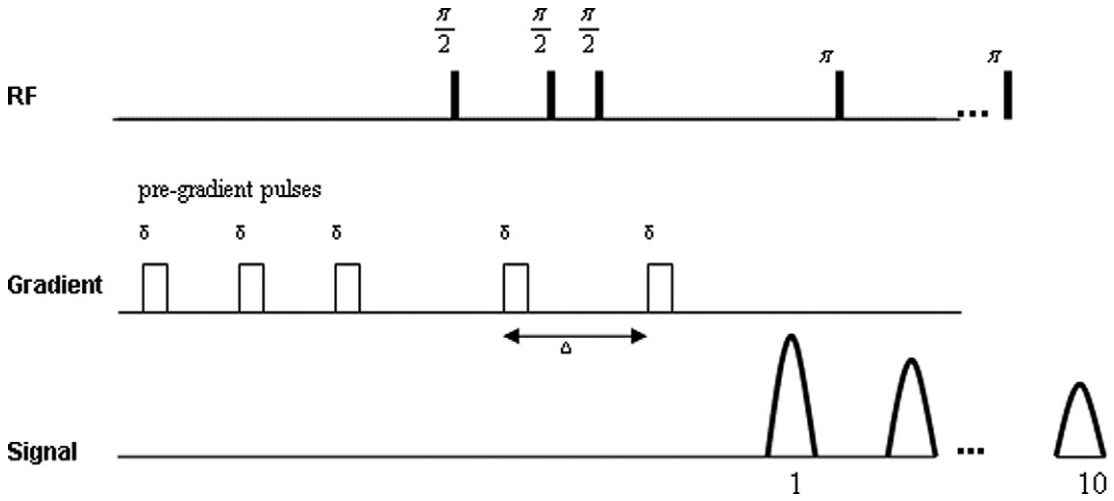

Fig. 2. Pulsed field gradient (PFG) pulse sequence with stimulated echoes and pre-gradient pulses. The amplitudes of the first 10 echoes are fit by linear regression to obtain the amplitude of the first echo.

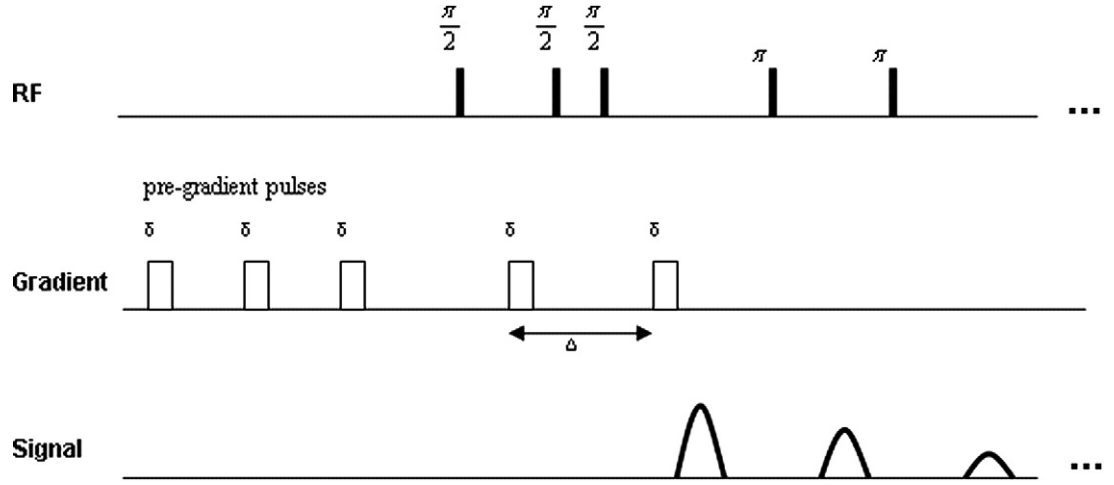

Fig. 3. Pulsed field gradient with diffusion editing (PFG-DE) pulse sequence.

phases [6].

$$R_{\text{emul}} = (1-\kappa)R_{\text{DP}} + \kappa R_{\text{CP}}, \quad 0 \leqslant \kappa \leqslant 1.0. \tag{5}$$

The fraction of the attenuation from the continuous phase is given by the parameter, κ.

$$\kappa = \left[1 + \frac{\sum(f_i)_{\text{DP}} \exp\left[\frac{-(\Delta+\tau)}{(T_{2,i})_{\text{DP}}}\right]}{\sum(f_i)_{\text{CP}} \exp\left[\frac{-(\Delta+\tau)}{(T_{2,i})_{\text{CP}}}\right]}\right]^{-1}. \tag{6}$$

The $T_{2,i}$ and f_i values are obtained from a CPMG measurement. The time between the first and second $\pi/2$ pulses is τ. The attenuation of the continuous phase, R_{CP}, is given by

$$R_{\text{CP}} = \exp\left(-\gamma_g^2 g^2 D_{\text{CP}} \delta^2 \left(\Delta - \frac{\delta}{3}\right)\right). \tag{7}$$

The attenuation of the dispersed phase, R_{DP}, is given by equation [9]

$$R_{\text{DP}} = \frac{\int_0^\infty p(r) R_{\text{sp}(r)}\, \mathrm{d}r}{\int_0^\infty p(r)\, \mathrm{d}r}. \tag{8}$$

The volume weighted drop size distribution, $p(r)$, is the log-normal probability density function [19]:

$$p(r) = \frac{1}{2r\sigma(2\pi)^{1/2}} \exp\left(-\frac{(\ln(2r) - \ln(d_v))^2}{2\sigma^2}\right). \tag{9}$$

The volume weighted mean is given by d_v and the width of the distribution is σ.

The PFG technique involves obtaining attenuation of the signal as a function of gradient strength and subsequently fitting the experimental attenuation to the predicted attenuation according to the restricted diffusion model. For this work, a nonlinear least squares algorithm with optimization was used to perform the fitting (lsqcurvefit in MatLab 7.1, The MathWorks Inc.).

2.3. Pulsed field gradient with diffusion editing (PFG-DE)

Fig. 3 shows that the standard PFG pulse sequence that was previously discussed can be modified to include several thousand 180° pulses at the end of the gradient sequence to gather transverse relaxation information [13,14].

Similar to the standard PFG technique, the gradient values are manipulated to facilitate attenuation due to restricted diffusion. However, the PFG-DE technique acquires thousands of echoes, thus resulting in the attainment of both diffusion and transverse relaxation information.

Flaum derived the magnetization equation that is used to characterize restricted diffusion of spheres and transverse relaxation simultaneously [13]:

$$M(g,t) = \iint f(r,T_2)\exp\left(-\frac{t}{T_2}\right)R_{\mathrm{sp}}(\Delta,\delta,g,r) \times \exp\left(-\frac{\Delta+\delta}{T_1} - 2\delta\left(\frac{1}{T_2}-\frac{1}{T_1}\right)\right)\mathrm{d}r\,\mathrm{d}T_2. \quad (10)$$

The longitudinal relaxation time, T_1, was assumed to be equal to T_2 in this work, which is a valid assumption for liquids at 2 MHz [22]. The attenuation of the brine drops according to Eqs. (2)–(4) is given by R_{sp}. The distribution of both drop size and transverse relaxation, $f(r,T_2)$, is determined using a two-dimensional inversion with regularization [13–15].

2.4. Parameter selection

The parameters that are used in both the PFG and PFG-DE techniques are obtained by solving the series model for restricted diffusion in spheres given by Murday and Cotts [11,13]. Specifically, the primary parameters that affect both the PFG-DE and PFG measurements are the time between gradient pulses (Δ), gradient duration (δ), and gradient strength (g). Both physical and equipment constraints must be accounted for when determining the parameters for a given experiment. Selection of Δ must be made based on the range of sizes of the drops expected in the sample and the SNR of the system. To distinguish restricted diffusion from free diffusion, the dimensionless time between gradient pulses must be greater than or equal to 1.0 [13]:

$$\frac{2D_{\mathrm{DP}}\Delta}{r^2} \geqslant 1.0. \quad (11)$$

If Δ is too small, the measurement will not be sensitive to large drops. If Δ is too large, the SNR will be low because of T_2 relaxation of the drops:

$$\frac{r^2}{2D_{\mathrm{DP}}} \leqslant \Delta \leqslant 0.3T_{2,\mathrm{DP}}. \quad (12)$$

Therefore, to investigate the largest possible sphere sizes, Δ must be as large as possible but less than a fraction of the dispersed phase transverse relaxation time. After Δ is established, the gradient duration, δ, is calculated. The minimum value of the gradient duration is instrument specific, and the maximum value is based on an established rule of thumb [13]:

$$\delta_{\min} \leqslant \delta \leqslant 0.2\Delta. \quad (13)$$

With the gradient spacing and duration calculated, the gradient values that achieve the desired attenuation can be calculated using the previously described series model for restricted diffusion in spheres. Ideally, for a given sphere size, the attenuation should range from 0.99 to 0.01 [13].

Fig. 4 illustrates the relationship between the parameters in a given experiment. In the top figure, the solid curve shows the T_2 distribution of the dispersed fluid. The dashed curve is the time between the two gradient pulses in the pulse sequence, Δ, and the dotted curve is the gradient duration, δ. The minimum time between gradient pulses, $\Delta_{\min}$, is shown as the dashed-dotted line in the top figure. When the calculated Δ falls below $\Delta_{\min}$, the measurement is no longer sensitive to restricted diffusion, thus resulting in the maximum detectable drop size, $r_{\max}$. The minimum detectable drop size, $r_{\min}$, is calculated based on the maximum gradient duration and maximum gradient strength of

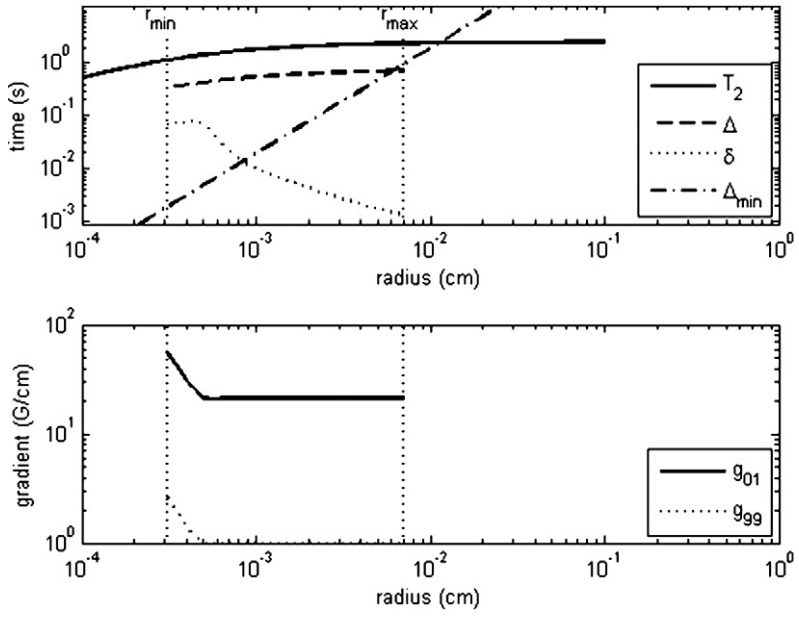

Fig. 4. Example of parameters calculated for PFG-DE and PFG measurements. These parameters were calculated with: $\rho = 1.0$ μm/s, $D_{\mathrm{brine}} = 2.6 \times 10^{-9}$ m^2/s, $T_{2,\mathrm{bulk}} = 2.5$ s, and $\Delta/T_{2,\mathrm{DP}} = 0.3$.

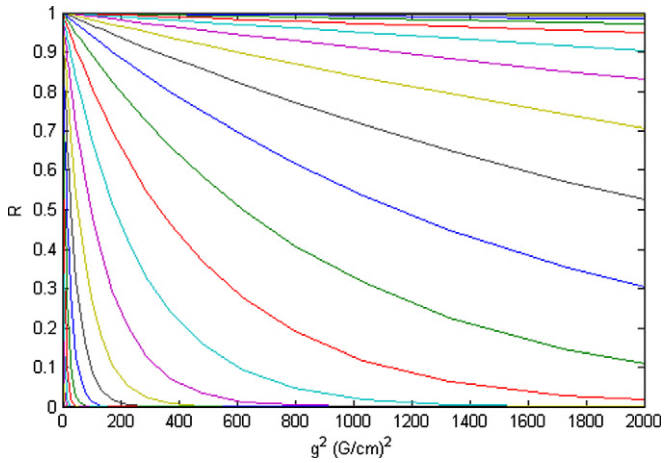

Fig. 5. Attenuation of 60 drop sizes using one parameter set ($\Delta = 244$ ms, $\delta = 49$ ms, $g = 2$–47 G/cm).

the instrument. Finally, the bottom figure contains the range of gradient values that should be used to facilitate the desired amount of attenuation ranging from 1% signal remaining, g_{01}, to 99% signal remaining, g_{99}. In this work, 20–25 logarithmically spaced gradient values were calculated for each parameter set. If the drop size range of the system is not known before the measurement, one PFG measurement can be performed which gives an estimate of the range of drop sizes in the system.

For all PFG-DE measurements discussed in this paper, 32 scans were applied, 15,360 echoes were collected with the echo spacing equal to 600 μs, and the relaxation delay was equal to 10 s. With these parameters, a typical measurement required 5–7 h for each parameter set. The PFG-DE technique is not affected by sedimentation of the drops in the emulsion; however, the technique is sensitive to coalescence. Therefore, the PFG-DE technique is applicable to emulsions that resist coalescence for many hours [1–3,20,21]. Though this work is focused on brine/crude oil emulsions, oil/water emulsions could also be investigated using the PFG-DE technique with the described parameter selection method. A possible problem that could occur with oil/water emulsions is that Δ might be required to be long to characterize larger drops, thus resulting in a significant loss of signal due to T_2 relaxation of the oil.

Using a technique developed by Flaum [13], multiple sets of parameters can be used to characterize a given drop size range. This technique, referred to as masking, incorporates multiple parameter sets with each set optimized for a particular radius and consisting of one Δ value, one δ value, and a logarithmically spaced list of gradient strength values. For drop size masking, the masking technique weights the most sensitive drop size range of each parameter set based on the attenuation imparted by the parameter set and the SNR of the measurement. Fig. 5 shows the attenuation curves that were obtained with $\Delta = 244$ ms, $\delta = 49$ ms, and $g = 2$–47 G/cm.

Each curve in Fig. 5 represents the attenuation imparted by a given parameter set to fluids diffusing in a given sphere size. In this figure, the attenuation curves from 60 different radii logarithmically spaced between 1×10^{-5} and 0.1 cm are displayed.

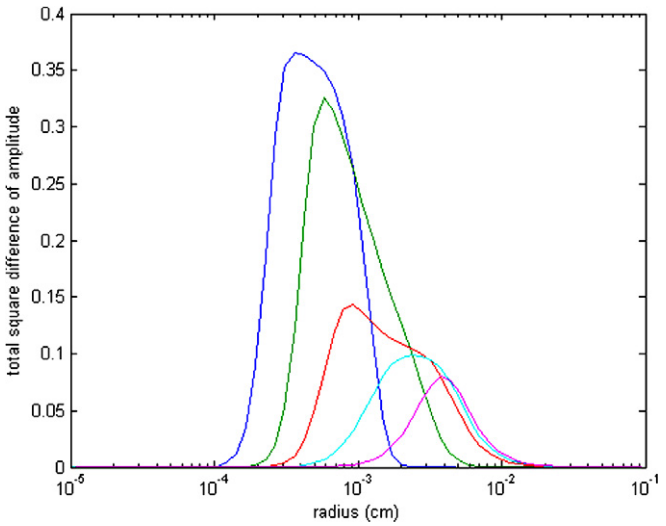

Fig. 6. Sensitivity of five parameter sets.

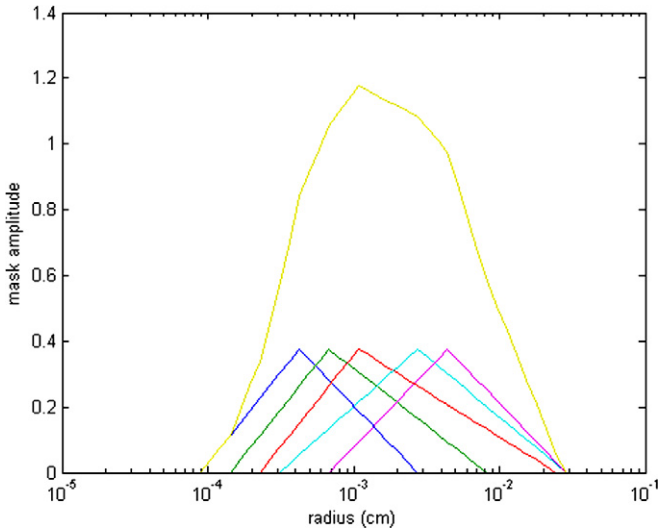

Fig. 7. Drop size masks for each parameter set.

The attenuation for each parameter set can be used to determine the sensitivity of each parameter set. Fig. 6 illustrates the determination of the sensitive region of each parameter set by plotting the sums of the square differences of attenuation between each drop size and the two adjacent drop sizes for five parameter sets.

At each gradient value, the attenuation of one sphere size is compared to the attenuation of the two adjacent sphere sizes to ensure that the sphere sizes can be distinguished. The limit of each parameter set is dictated by the noise of the measurement:

$$\text{cutoff} = 2(\sigma_{\text{noise}})^2 N_{\text{grad}}. \tag{14}$$

In this equation, the standard deviation of the noise is given by σ_{noise} and the number of gradients is given by N_{grad}. The intersections of the value obtained from Eq. (14) with the sensitivity curves in Fig. 6 designate the boundaries of the sensitivity of each parameter set. For this example, the cutoff was calculated to be 0.001, resulting in Fig. 7.

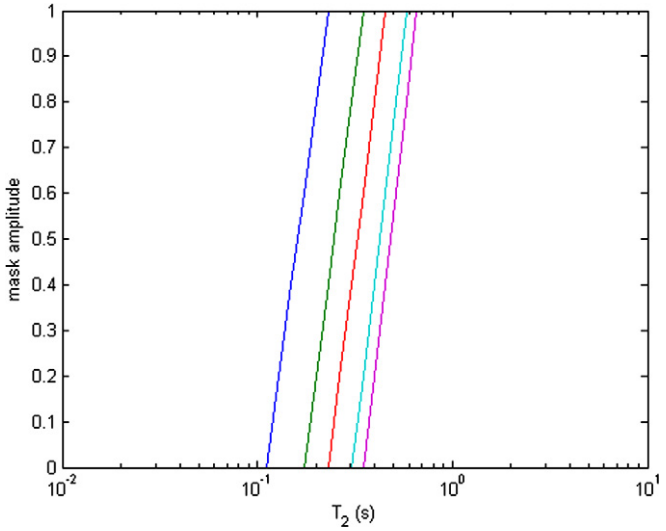

Fig. 8. T_2 masking for five parameter sets.

Table 1
Experimental NMR parameters

Experiment	$d_{optimal}$ (μm)	Δ (ms)	δ (ms)	g (G/cm)	d_{range} (μm)
1	20	598	5.7	1–10	10–140
2	10	552	28	1–13	5–60
3, first set	10	470	28	1–15	5–70
3, second set	20	598	5.7	1–10	10–140

The masks have maximum amplitude at the radii for which the parameters are most sensitive, and the range extends to the boundaries of the sensitivity of each parameter set as determined by Eq. (14). The masked drop size distribution is a weighted sum of the drop size distribution obtained from each parameter set divided by the amplitude of the combined mask.

Similarly, the transverse relaxation distribution is masked according to Δ. In this work, transverse relaxation times shorter than half of Δ were masked. The masking proceeds linearly in log T_2 until the value of Δ is reached as shown in Fig. 8 for five parameter sets.

Any component that has a relaxation time significantly faster than Δ will have relaxed substantially before the first echo is collected. In this work, components that relaxed faster than 0.5 times Δ were masked which corresponded to a decrease in signal amplitude of 85%. The fast relaxing crude oil components were the only species affected by the T_2 masking in this work.

Table 1 contains the NMR parameters that were calculated for each of the three experiments discussed in this paper. Experiments 1 and 2 each required one set of parameters while the third experiment required two parameter sets.

2.5. Emulsion preparation

The emulsions considered in this work were prepared using a Couette flow device. The rotating, inner cylinder was composed of Torlon with radius, $r_T = 19.1$ mm. The stationary, outer cylinder was composed of glass with radius, $r_g = 21.6$ mm. The rotational speed of the inner cylinder was adjusted depending on the desired experimental conditions, and the shear rate is given by

$$\gamma = \frac{2\pi\omega r_T}{(r_g - r_T)}. \tag{15}$$

The rotational speed of the inner cylinder is given by ω. Shear rates ranged from 1.3×10^3 to 3.2×10^3 s^{-1}, depending on the experiment. Each emulsion was sheared for 10 min.

The sample temperatures were not measured during the NMR measurements. However, all samples were placed into a temperature controlled spectrometer at 30 ± 0.1 °C during the NMR measurements. For all of the emulsions discussed, the dispersed phase was ASTM certified synthetic seawater. Two different crude oils were used for the continuous phase, denoted as either crude oil A or crude oil B. Table 2 contains density and viscosity information for the crude oils.

Table 2
Density and viscosity information for the two crude oils used in this work

Crude oil	Density (g/mL)	Viscosity (cP)
A	0.85	15.0
B	0.81	2.0

Table 3
Summary of formation conditions and measurement durations for the three experiments

Experiment	γ (s^{-1})	Shear duration (min)	Measurement duration (h)
1	1.3×10^3	10	7
2	3.2×10^3	10	7
3	$1.3 \times 10^3, 2.3 \times 10^3$	10, 10	25

Each emulsion discussed in this paper contained 20 vol% brine and 80 vol% crude oil. After forming each emulsion, the glass sample vessel containing the emulsion was placed in the spectrometer. Table 3 summarizes the formation conditions and measurement durations for the three experiments presented in this work.

3. Results

The following sections contain three different cases that show the usefulness of the PFG-DE technique. The first case illustrates a situation when the T_2 distribution of the emulsified brine overlaps the bulk brine T_2 distribution. The second case illustrates the situation when the T_2 distribution of the emulsified brine overlaps the T_2 distribution of the crude oil. Finally, the third case illustrates the ability of the PFG-DE technique to resolve a bimodal drop size distribution.

3.1. Emulsified brine T_2 distribution overlaps the bulk brine T_2 distribution (Experiment 1, crude oil A)

Drop size distributions of brine/crude oil A emulsions were obtained using the CPMG, PFG-DE, and PFG techniques. Fig. 9 shows the T_2 distribution of an emulsion that was formed by combining 10 mL of brine with 40 mL of crude oil A. Shear was applied to the emulsion with $\gamma = 1.3 \times 10^3$ s^{-1}.

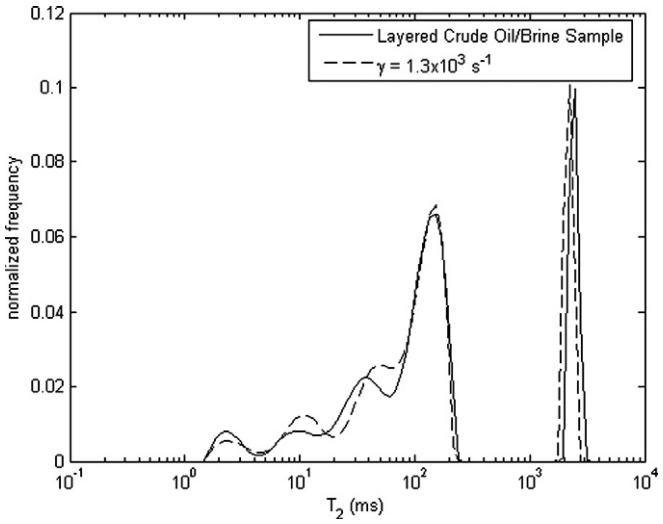

Fig. 9. T_2 distribution of an emulsion with $\gamma = 1.3 \times 10^3\ s^{-1}$ for 10 min. Note the proximity of the emulsified brine T_2 distribution to the bulk brine T_2 distribution.

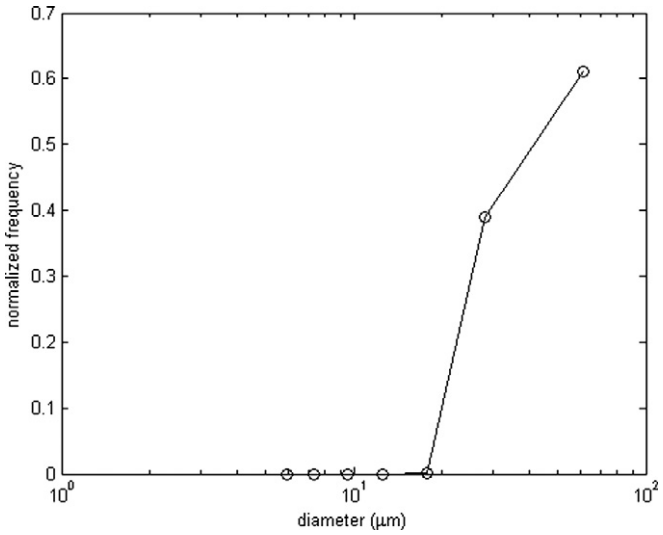

Fig. 10. Drop size distribution obtained from transverse relaxation data. Note the increase in the width of the distribution that was caused by the approach of the emulsified brine T_2 distribution to the bulk brine T_2 distribution.

Fig. 9 shows the overlap of the emulsified brine T_2 distribution and the bulk brine T_2 distribution. Fig. 10 shows the drop size distribution that was obtained by using the emulsified brine T_2 distribution in conjunction with Eq. (1).

The drop size distribution in Fig. 10 illustrates the error that is introduced when using Eq. (1) if the T_2 distribution of the emulsified brine is close to the bulk brine T_2 distribution. Equation (1) assumes that the transverse relaxation distribution of the bulk brine is single valued. Experimentally, the bulk brine exhibits a finite range of T_2 values. Therefore, the emulsified brine can overlap the bulk brine distribution, thus causing a significant increase in the uncertainty of the drop size distribution. In addition, Eq. (1) requires the use of the surface relaxivity, which was obtained from

$$\rho = \frac{d_v}{6}\left(\frac{1}{T_{2,\text{emulsified brine}}} - \frac{1}{T_{2,\text{bulk}}}\right). \tag{16}$$

The volume weighted mean diameter, d_v, and the log mean T_2 value of the emulsified brine, $T_{2,\text{emulsified brine}}$, were obtained from a PFG-DE measurement. For this brine/crude oil system, the surface relaxivity was determined to be 0.5 μm/s.

The PFG-DE and PFG techniques were performed on the same emulsion. With the input values of $T_{2,\text{bulk}} = 2.5$ s, $\rho = 0.5$ μm/s, and $\Delta / T_{2,\text{DP}} = 0.3$, the following parameters were calculated, as shown in Table 1, based on the previously discussed parameter selection method: $\Delta = 598$ ms, $\delta = 5.7$ ms, and $g = 1$–10 G/cm. These parameters were calculated to be sensitive to drop diameters in the range, 10–140 μm.

Unlike the CPMG technique, the PFG-DE technique does not rely on the T_2 distribution to generate the drop size distribution. Fig. 11 contains the two-dimensional map that was generated using the PFG-DE technique.

The emulsified brine and crude oil A contributions are separated with respect to the T_2 distribution, thereby making the drop size distribution only dependent on the brine contribution. In addition, the T_2 relaxation contribution from the crude oil has been minimized as a result of the choice of the gradient spacing. The PFG technique was performed to confirm the drop size distribution obtained from the PFG-DE technique, and the results are shown in Fig. 12.

The drop size distributions shown in Fig. 12 are summarized by quantifying the volume weighted mean diameter, d_v, and one standard deviation on either side of the volume weighted mean diameter, $\{\frac{d_v}{e^\sigma}, d_v, d_v e^\sigma\}$. Because the PFG-DE technique yields a discrete drop size distribution and the PFG technique yields a continuous probability density function, a relationship must be established between the results of the two techniques to graphically compare the two techniques. The cumulative distribution can be written according to

$$P(d_i) = \sum_{j=1}^{j=i} f_j. \tag{17}$$

The normalized frequency obtained from the PFG-DE technique is given by f_j. Because the probability density function for the PFG technique is assumed to be lognormal with equal increments of the logarithm of the diameter, the cumulative distribution can further be written in terms of the normalized frequency from the PFG-DE technique:

$$\Delta P_i = d_i\, p(d_i) \Delta\big(\log(d_i)\big) = f_i. \tag{18}$$

The probability density function for the PFG technique is denoted by $p(d_i)$. Unlike the CPMG technique as shown in Fig. 10, the PFG-DE and PFG techniques have the ability to resolve the drop size distribution when the T_2 distribution of the emulsion overlaps the bulk brine T_2 distribution.

3.2. Emulsified brine T_2 distribution overlaps the bulk crude oil T_2 distribution (Experiment 2, crude oil B)

If the T_2 distribution of the emulsified brine overlaps the T_2 distribution of the crude oil in the emulsion, the transverse relaxation data cannot be used to obtain the drop size distribution of the emulsion. An emulsion was prepared by combining 5 mL

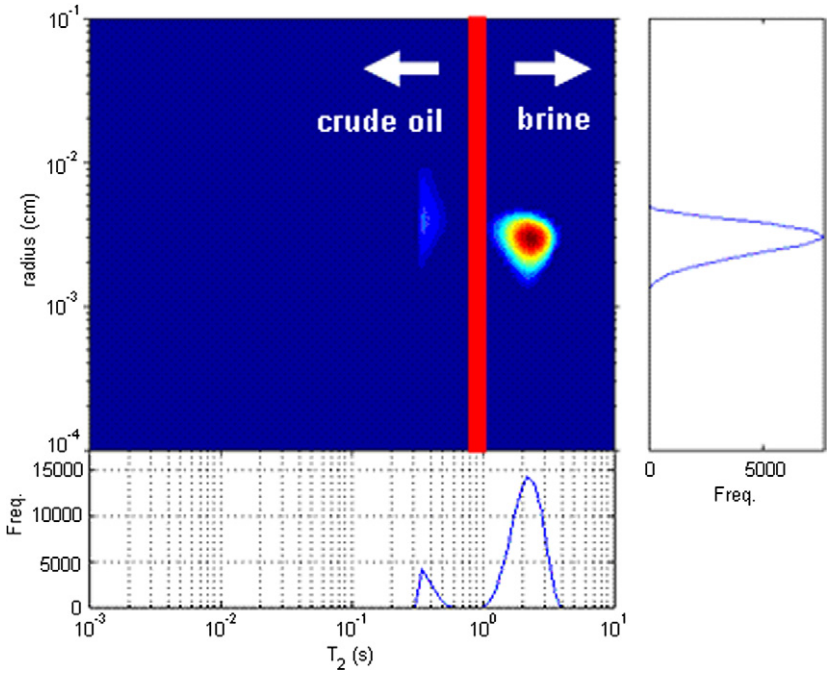

Fig. 11. Two-dimensional map produced from the PFG-DE technique after application of the mask. Note the separation of the crude oil A and brine in terms of transverse relaxation. Only brine contributes to the drop size distribution.

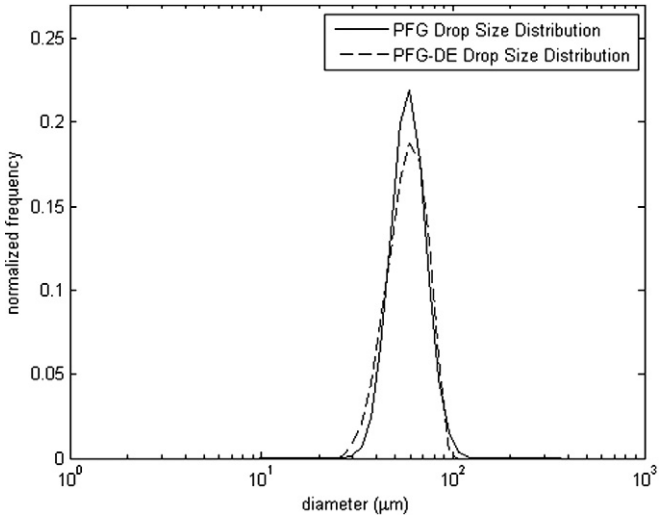

Fig. 12. Comparison of drop size distributions obtained from the PFG-DE and PFG techniques. The drop size distribution from the PFG-DE technique given by the mean and one standard deviation on either side of the mean {45, 59, 72} μm agrees well with the traditional PFG technique, {47, 58, 72} μm.

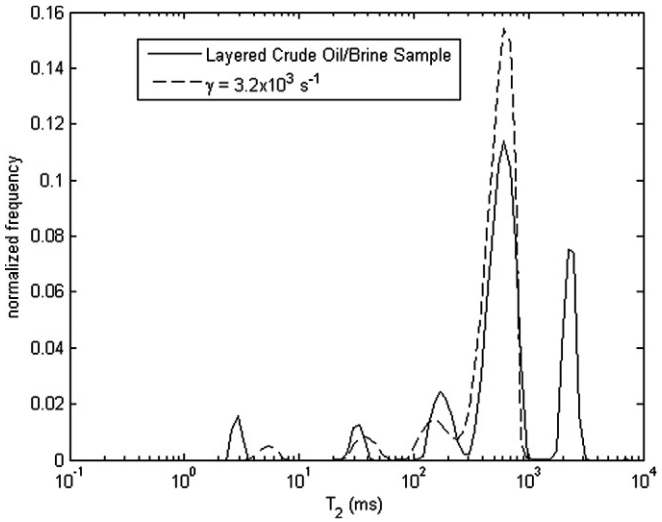

Fig. 13. Overlap of emulsion and crude oil B T_2 distributions.

of brine with 20 mL of crude oil B. The emulsion was sheared for ten minutes with $\gamma = 3.2 \times 10^3\ s^{-1}$. Fig. 13 shows the overlap of the emulsified brine and crude oil T_2 distributions.

The solid curve in Fig. 13 is the T_2 distribution of the layered crude oil B/brine sample, and the dashed curve is the T_2 distribution of the emulsion. Because the emulsified brine and crude oil B T_2 distributions are not separable, Eq. (1) cannot be used to calculate the drop size distribution.

The parameters for the PFG-DE technique were calculated based on ($T_{2,\text{bulk}} = 2.5$ s, $\rho = 0.3$ μm/s, and $\Delta/T_2 = 0.3$), and the values were: $\Delta = 552$ ms, $\delta = 28$ ms, and $g = 1$–13 G/cm, as shown in Table 1. The parameters were sensitive to drop diameters in the range, 5–60 μm. The two-dimensional map obtained from the PFG-DE technique after applying the masking technique is shown in Fig. 14.

Fig. 14 shows that the drop size distribution of the brine phase was extracted using the PFG-DE technique even though the T_2 distributions of the emulsified brine and crude oil B overlap. The lack of contribution of the crude oil B to the drop size distribution is evident when considering the attenuation of the emulsion as shown in Fig. 15.

Fig. 15 shows that the crude oil B does not significantly contribute to the attenuation of the signal of the emulsion based on Eq. (7). The signal of the crude oil B is negligible after the sec-

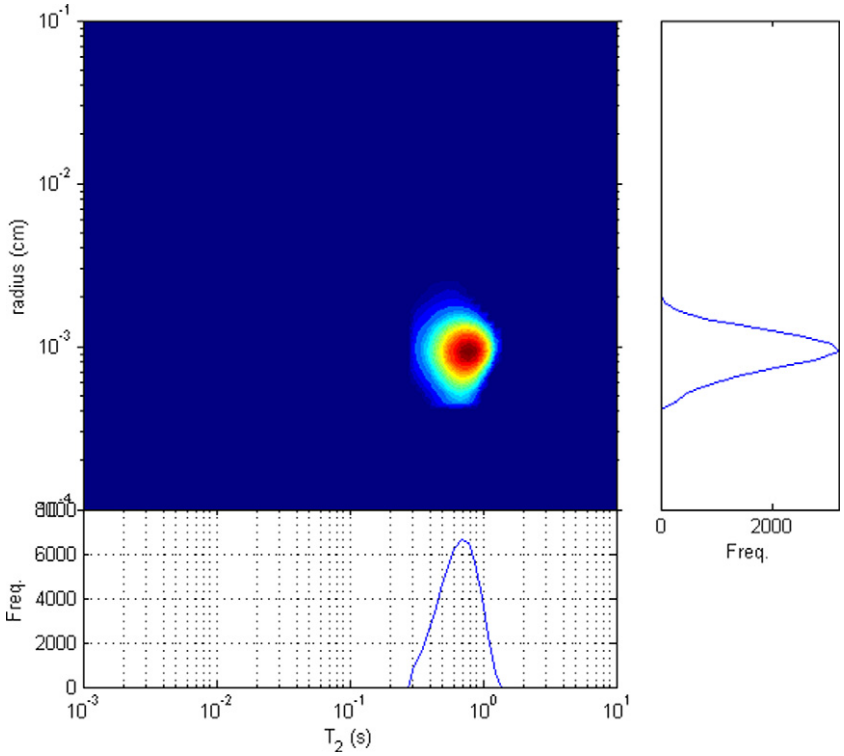

Fig. 14. Two-dimensional map of brine/crude oil B emulsion after masking. The emulsified brine and crude oil B T_2 distributions overlap, but the crude oil B does not contribute to the drop size distribution because the crude oil B signal attenuated significantly.

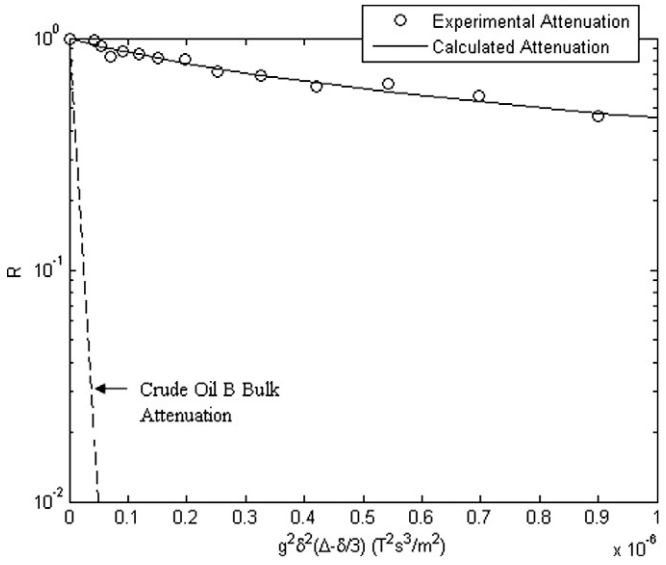

Fig. 15. Experimental and predicted attenuation for the Experiment 2 brine/crude oil B emulsion ($\Delta = 552$ ms, $\delta = 28$ ms, and $g = 1$–13 G/cm). Note that the crude oil B does not contribute to the attenuation of the signal of the emulsion, thereby facilitating the separation of the crude oil B and brine contributions.

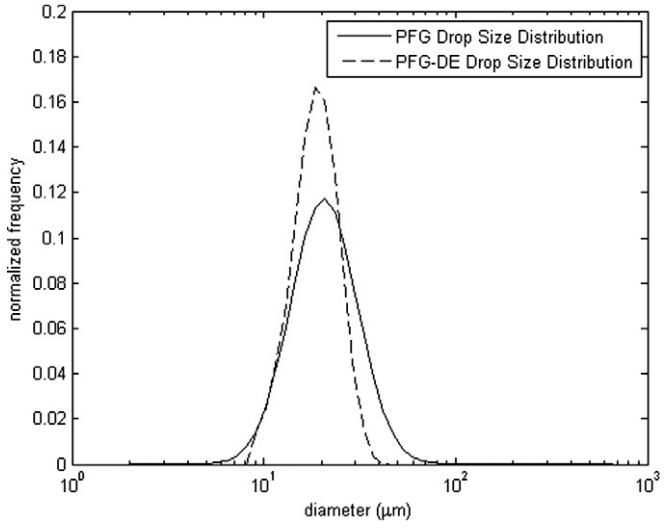

Fig. 16. Comparison of drop size distributions obtained from the PFG-DE and PFG techniques. The drop size distribution from the PFG-DE technique, {14, 19, 24} μm, agrees well with the traditional PFG technique {14, 21, 31} μm.

ond gradient pulse; therefore, the emulsified brine and crude oil B contributions can be separated. As shown by Peña [6], if the signal from the continuous phase is diminished, only the brine signal contributes to the determination of the drop size distribution. Though the oil signal does not have to be eliminated to use Eq. (10), the effective diffusivities of the brine and crude oil must be separable to effectively characterize the emulsified brine drop size distribution.

The PFG measurement was performed using the same parameters as those used for the PFG-DE measurement, and the comparison of the drop size distributions is shown in Fig. 16.

Table 4 contains a summary of the results for the two previously described experiments.

Table 4
Summary of results for the unimodal brine/crude oil emulsions

Experiment	Method	γ (s^{-1})	$-\sigma$ (μm)	d (μm)	$+\sigma$ (μm)
1	PFG-DE	1.3×10^3	45	59	72
1	PFG	1.3×10^3	47	58	72
2	PFG-DE	3.2×10^3	14	19	24
2	PFG	3.2×10^3	14	21	31

3.3. Bimodal drop size distribution (Experiment 3, crude oil A)

The PFG-DE technique is particularly useful for determining the drop size distribution when the emulsion contains a bimodal drop size distribution. A bimodal drop size distribution was prepared by combining two independently formed emulsions. One emulsion was prepared by shearing 10 mL of brine with 40 mL of crude oil A. The shearing duration was 10 min with $\gamma = 2.3 \times 10^3$ s^{-1}. An independent emulsion consisting of 10 mL of brine and 40 mL of crude oil A was formed with $\gamma = 1.3 \times 10^3$ s^{-1} and shearing duration equal to 10 min. The PFG-DE and PFG measurements were performed on both of the independent emulsions. From each independent emulsion, 25 mL was removed and combined into one glass sample vessel to form a bimodal drop size distribution. The PFG-DE measurement was performed on the combined emulsion.

By applying two different shear rates, it was expected that two different populations of drops would form. Therefore, two different parameter sets were constructed to characterize the two different drop size distributions. With $\gamma = 2.3 \times 10^3$ s^{-1}, parameters were calculated with maximum sensitivity to drops with diameters equal to 10 μm in the range (5–70 μm). To characterize this range of diameters, the following parameters were calculated using the previously described algorithm based on $T_{2,\text{bulk}} = 2.5$ s, $\rho = 0.5$ μm/s, and $\Delta/T_2 = 0.3$: $\Delta = 470$ ms, $\delta = 28$ ms, $g = 1$–15 G/cm. The PFG technique was also used to measure the drop size distribution of the emulsion, and the comparison is shown in Fig. 17.

Fig. 17 shows the agreement that was achieved between the PFG-DE technique and the PFG technique with $\gamma = 2.3 \times 10^3$ s^{-1}.

With $\gamma = 1.3 \times 10^3$ s^{-1}, parameters were calculated with maximum sensitivity to drops with diameters equal to 20 μm in the range (10–140 μm). To characterize this range of diameters, the following parameters were calculated using the previously described algorithm based on $T_{2,\text{bulk}} = 2.5$ s, $\rho = 0.5$ μm/s, and $\Delta/T_2 = 0.3$: $\Delta = 598$ ms, $\delta = 5.7$ ms, $g = 1$–10 G/cm. The PFG technique was also used to measure the drop size distribution of the emulsion, and the comparison is shown in Fig. 18.

Fig. 18 shows the agreement that was achieved between the PFG-DE and PFG techniques with $\gamma = 1.3 \times 10^3$ s^{-1}.

An emulsion with a bimodal drop size distribution was formed by combining 25 mL of the emulsion with $\gamma = 2.3 \times 10^3$ s^{-1}, with 25 mL of the emulsion with $\gamma = 1.3 \times 10^3$ s^{-1}. The PFG-DE measurement of the bimodal emulsion consisted of two complete parameter sets: [$\Delta = 470$ ms, $\delta = 28$ ms, $g = 1$–15 G/cm] and [$\Delta = 598$ ms, $\delta = 5.7$ ms, $g = 1$–10 G/cm].

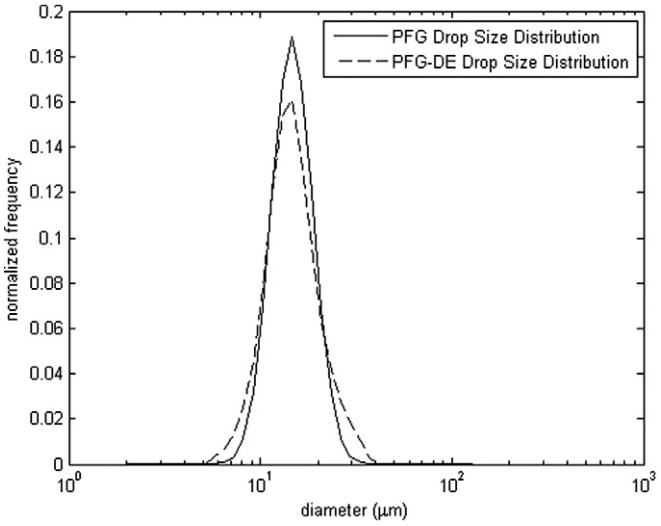

Fig. 17. Comparison of drop size distributions with $\gamma = 2.3 \times 10^3$ s^{-1}. The PFG-DE technique yielded a drop size distribution, {10, 15, 20} μm, that agreed with the PFG technique, {11, 15, 19} μm.

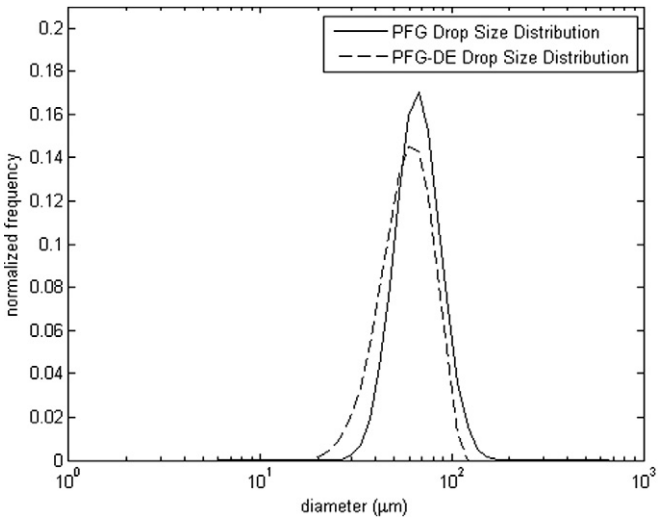

Fig. 18. Comparison of drop size distributions with $\gamma = 1.3 \times 10^3$ s^{-1}. The PFG-DE technique yielded a drop size distribution, {42, 60, 78} μm, that agreed with the PFG technique, {50, 66, 87} μm.

The masking technique developed by Flaum [13] was used to investigate the range of sizes of the bimodal distribution as described in Section 2.4. The sensitivity for each parameter set is given in Fig. 19.

The drop size masks were determined based on the sensitivity of each parameter set and the noise cutoff of the measurement which was 0.02 for this experiment. The limits of each parameter set as a result of the noise are given in Fig. 20.

Fig. 21 shows the limits of the sensitivity of the first parameter set.

The solid line indicates the most sensitive drop size of the measurement, and the dashed lines indicate the limits of the sensitivity of the measurement. Similarly, the sensitivity of the second parameter set is shown in Fig. 22.

The second parameter set is sensitive to the larger population of drop sizes as shown in Fig. 22.

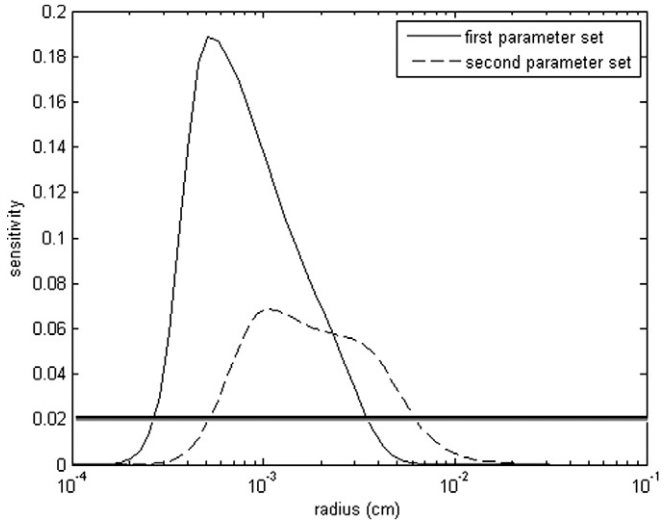

Fig. 19. Sensitivity of the two parameter sets with the noise cutoff equal to 0.02.

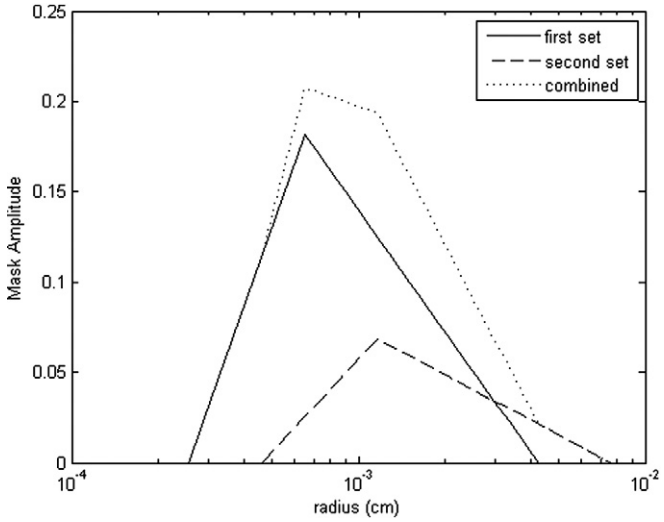

Fig. 20. Drop size masks for each parameter set.

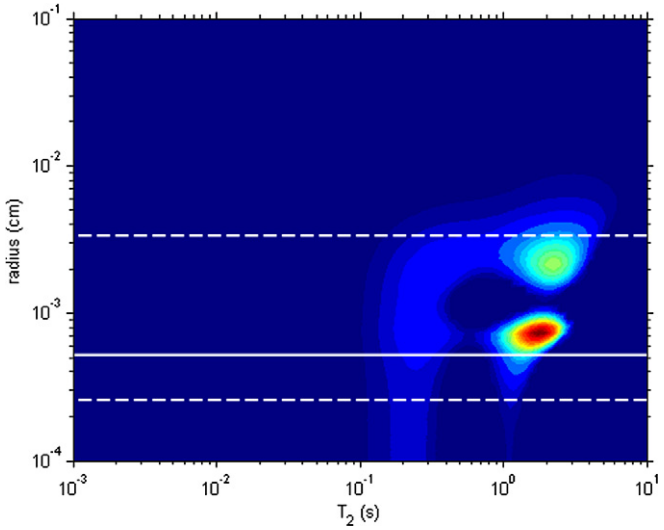

Fig. 21. Two-dimensional results for the first parameter set. The most sensitive drop size is indicated by the solid line while the limits of the sensitivity of the measurement are indicated by the dashed lines. Note that the population of smaller drops exists in the sensitive region.

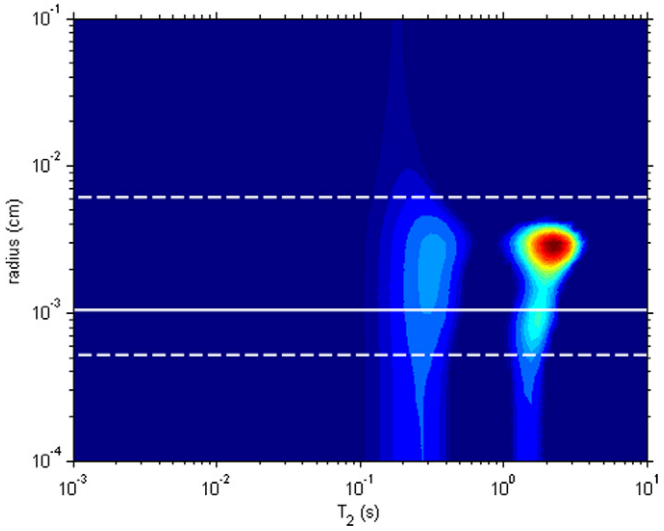

Fig. 22. Two-dimensional results for the second parameter set. Note that the larger population of drop sizes is present in the sensitive region.

In addition to masking the measurement according to the drop size, the masking procedure also applies to the transverse relaxation distribution. As discussed in Section 2.4, all transverse relaxation times that are less than half of Δ are masked. Fig. 23 shows that transverse relaxation times less than 250 ms were masked for this example.

For this example, masking the transverse relaxation merely diminishes the transverse relaxation contribution of the crude oil while the emulsified brine contribution is unaffected. Fig. 24 shows the final result after masking both drop size and transverse relaxation.

The crude oil A and brine contributions were isolated according to the separation in terms of the T_2 distributions, and the resulting bimodal drop size distribution is given in Fig. 25.

Fig. 25 illustrates the ability of the PFG-DE technique to resolve the bimodal drop size distribution. The independently measured unimodal drop size distributions of each emulsion are plotted in conjunction with the bimodal drop size distribution. Fig. 25 shows that the first population of sizes in the bimodal distribution, {11, 14, 17} μm, agrees with the PFG-DE measurement of the corresponding unimodal drop size distribution, {10, 15, 20} μm. In addition, the second population of drop sizes in the bimodal distribution, {39, 52, 65} μm, also agrees with the PFG-DE measurement of the corresponding unimodal distribution, {42, 60, 78} μm. These results show that the PFG-DE technique has the ability to resolve a bimodal drop size distribution which is in agreement with the independent, unimodal drop size distributions.

4. Conclusion

Based on the work presented in this paper, the PFG-DE technique has the ability to resolve drop size distributions of emulsions in different physical situations. In addi-

tion, the parameter selection algorithm developed by Flaum [13] facilitates accurate measurements of drop size distributions of emulsions. The results from the PFG-DE technique have been shown to agree with the traditional PFG technique. The PFG-DE technique also has the ability to resolve more complicated drop size distributions such as bimodal drop size distributions. In general, the PFG-DE technique is useful because it provides both transverse relaxation and drop size distributions simultaneously, and it is not constrained by an assumed shape of the drop size distribution.

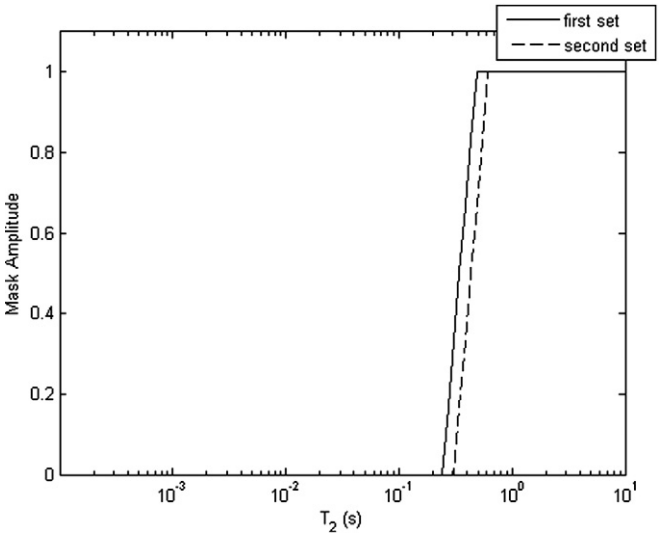

Fig. 23. Transverse relaxation masks for the two parameter sets.

Acknowledgments

The authors would like to thank Dick Chronister, Dr. Alberto Montesi, Dr. Jeff Creek, Dr. Waylon House, Michael Rauschhuber, and Chevron for financial support.

Supplementary information

Supplementary material for this article may be found on Science Direct, in the online version.

Please visit DOI:10.1016/j.jcis.2007.07.057.

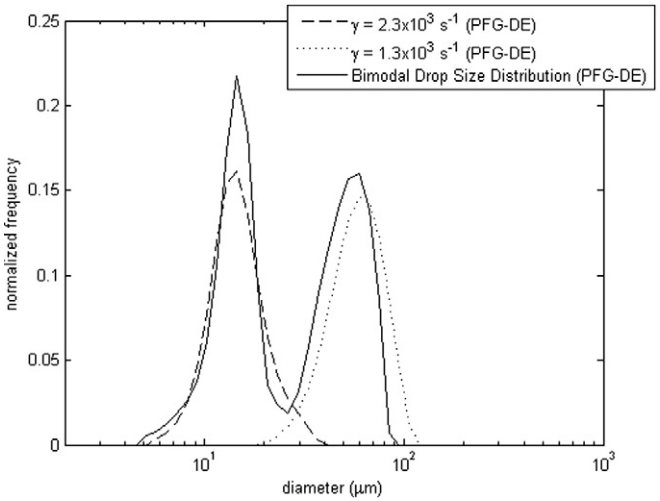

Fig. 25. Comparison of unimodal drop size distributions with the bimodal drop size distribution obtained using the PFG-DE technique.

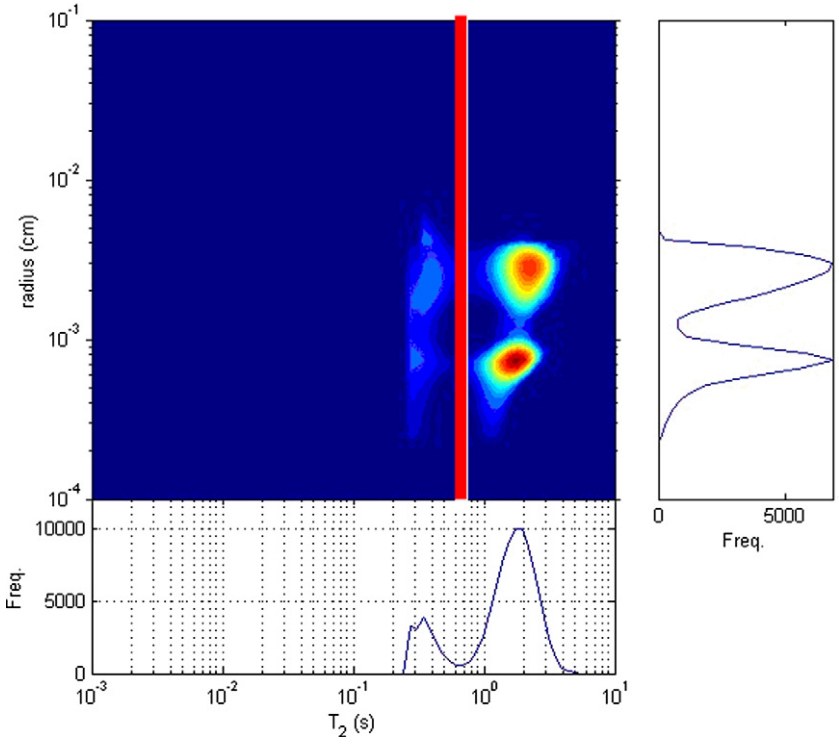

Fig. 24. Two-dimensional map of the bimodal drop size distribution after masking both drop size and transverse relaxation. The brine contribution to the drop size distribution was isolated according to the separation of the T_2 distributions.

References

[1] J. Sjöblom, P.V. Hemmingsen, H. Kallevik, in: O.C. Mullins, E.Y. Sheu, A. Hammami, A.G. Marshall (Eds.), Asphaltenes, Heavy Oils, and Petroleomics, Springer-Verlag, New York, NY, 2007, p. 549.

[2] L.L. Schramm, in: L.L. Schramm (Ed.), Emulsions: Fundamentals and Applications in the Petroleum Industry, in: Advances in Chemistry Series, vol. 231, American Chemical Society, Washington, DC, 1992, p. 1.

[3] P.K. Kilpatrick, P.M. Spiecker, in: J. Sjöblom (Ed.), Encyclopedic Handbook of Emulsion Technology, Dekker, New York, NY, 2001, p. 707.

[4] T. Skodvin, in: J. Sjöblom (Ed.), Encyclopedic Handbook of Emulsion Technology, Dekker, New York, NY, 2001, p. 695.

[5] P.V. Hemmingsen, X. Li, J.L. Peytavy, J. Sjöblom, J. Dispersion Sci. Technol. 28 (2007) 371.

[6] A. Peña, G.J. Hirasaki, in: J. Sjöblom (Ed.), Emulsions and Emulsion Stability, CRC, Boca Raton, FL, 2006, p. 283.

[7] P. Becher, Emulsions: Theory and Practice, Oxford Univ. Press, New York, NY, 2001.

[8] L.L. Schramm, Emulsions, Foams, and Suspensions: Fundamentals and Applications, Wiley–VCH, Weinheim/Great Britain, 2005.

[9] K.J. Packer, C. Rees, J. Colloid Interface Sci. 40 (1972) 206.

[10] C.H. Neuman, J. Chem. Phys. 60 (1974) 4508.

[11] J.S. Murday, R.M. Cotts, J. Chem. Phys. 48 (1968) 4938.

[12] A. Peña, G.J. Hirasaki, Adv. Colloid Interface Sci. 105 (2003) 103.

[13] M. Flaum, Fluid and Rock Characterization Using New NMR Diffusion-Editing Pulse Sequences and Two-Dimensional Diffusivity-T_2 Maps, Ph.D. thesis, Rice University, Houston, 2006.

[14] M.D. Hürlimann, L. Venkataramanan, J. Magn. Reson. 157 (2002) 31.

[15] L. Venkataramanan, Y.Q. Song, M.D. Hürlimann, IEEE Trans. Signal Process. 50 (2002) 1017.

[16] T. Garisanin, T. Cosgrove, Langmuir 18 (2002) 10298.

[17] H.Y. Carr, E.M. Purcell, Phys. Rev. 94 (1954) 630.

[18] S. Meiboom, D. Gill, Rev. Sci. Instrum. 29 (1958) 688.

[19] G. Casella, R.L. Berger, Statistical Inference, second ed., Duxbury, Pacific Grove, CA, 2002.

[20] J. Czarnecki, K. Moran, Energy Fuels 19 (2005) 2074.

[21] M.J. Rosen, Surfactants and Interfacial Phenomena, second ed., Wiley, New York, NY, 1989.

[22] P.T. Callaghan, Principles of Nuclear Magnetic Resonance Microscopy, Clarendon, New York, NY, 1991.